
# Computational modeling of steel fiber reinforced concrete

Victor Sloboda[1], Roberto Dalledone Machado[1,2], Ricardo Pieralisi[2]

[1]*Graduate Program in Numerical Methods in Engineering, UFPR – Paraná Federal University*
*100 Cel. Francisco H. dos Santos Avenue, Curitiba, PR, 81531-980, Brazil*
*victorsloboda@hotmail.com, roberto.dalledonemachado@gmail.com*
[2]*Graduate Program in Civil Construction Engineering, UFPR – Paraná Federal University*
*100 Cel. Francisco H. dos Santos Avenue, Curitiba, PR, 81531-980, Brazil*
*roberto.dalledonemachado@gmail.com, ricpieralisi@gmail.com*

**Abstract.** New building technologies are developed with the goal of improving structural performance. One very promising technology is the steel fiber reinforced concrete (SFRC), in which steel fibers are added in the concrete mixture. Concrete is a fragile material whose tensile resistance is very lower than compressive. Steel reinforcement, as well as steel fibers, improves the tensile behavior, grants more ductility to concrete and increases cracking and spalling resistance. Although SFRC is considered promising, there are still a few reliable computational models to analyze and predict the behavior of SFRC. The modeling is difficult because of the random distribution of fibers and the consequent anisotropy. A numerical and computational approaching, using numerical methods, is used to develop this work. Different constitutive models are analyzed and the results are compared with experimental data obtained from flexural tests. This work aims to extend the application of the SFRC in various situations, for example the precast structures.

**Keywords:** Concrete, Steel fiber, Modeling, Cracking.

## 1 Introduction

The idea of adding fibers in a material to improve its properties dates back to the ancient Egypt. According to Bentur and Mindess [1], the steel fiber reinforced concrete was invented in the 1960's. Concrete, the most used material in civil construction (Figueiredo [2]), is a versatile and low-cost material (Mehta et al. [3], Marchetti and Botelho [4]), however, it is brittle and has low tensile strength. Due to this shortcoming, steel bars, a material with high tensile strength, are added, resulting in reinforced concrete. Nonetheless, the cross sections of reinforced concrete are quite heterogeneous, whose zones of greatest tensile resistance are located in steel bar reinforcement. According to Kosmatka et al. [5], fibers, unlike steel bars, distribute the tensile stresses across the cross section of the structure, and can save the need of a frame sector at the construction worksite.

The goal of this work is to analyze how the addition of steel fibers can improve the behavior of concrete. This performance improvement is observed by modeling tests made in concrete structures, obtained with computational programs and numerical methods, mainly the Finite Element Method (FEM). After that, the results are compared with information from the literature or results recommended by the regulations.

The occurrence of catastrophic incidents, broadcast by media, involving the collapse of concrete structures, is one reason for choosing the addressed topic. Several critical incidents could be avoided or mitigated if the quality of the collapsed structures was better. The fibers can help slow down the crack growth or propagation and grant more ductility to the concrete, since the collapse is fragile and sudden.

Furthermore, cementitious materials with fibers are still underused, due mainly to the high cost and the decreasing in the workability of the mixture. Another reason is the relative insipience of this technology, mainly in Brazil, where research data on fiber reinforced concrete, as well as specific norms, is still lacking (Figueiredo [2]). Finally, the current constitutive models of the SFRC are not able to faithfully simulating the properties of the composite, due to the random distribution of the fibers (Bitencourt Jr et al. [6]).

## 2 Theoretical review

Fiber reinforced concrete is a wide subject and must be focused in different points of view, and therefore this work is supported by many references which concern with the theme. The overall of composite materials is addressed by Bentur and Mindess [1] and Jones [7]. The fiber reinforced concretes are well discussed by Bentur and Mindess [1], Figueiredo [2], Bitencourt Jr et al. [6], Blanco Álvarez et al. [8], Herscovici et al. [9], and PASA [10].

Blanco Álvarez et al. [8] approaches the modeling of steel-fiber reinforced concrete and obtaining the results of flexural tests, based on different European standard norms. Abeche [11] mentions the modeling and analysis of concrete structures considering the Damage Mechanics, emphasizing on dynamical analysis, which uses numerical and iterative methods (for instance, Newton-Raphson) to obtain the load-displacement curve. Opolski [12] focuses in nonlinear static analysis of reinforced concrete structures, also considering the Finite Element Method, the Newton-Raphson method and the Mechanics of Damage.

The normative FIB [13] is an international norm for fiber-reinforced concretes. The computational model for SFRC is a subject explored by PASA [10], Singh [14] and Kotsovos [15]. The Finite Element Method is approached by Soriano and Lima [16] and Oñate [17], and numerical methods of solving nonlinear equations are discussed by Bathe [18]. Finally, the normative NBR-6118:2014 (ABNT [19]) is a Brazilian norm for project of concrete structures.

### 2.1 Materials

The SFRC is a composite material consisted in concrete matrix and steel fibers (Jones [7]). Concrete is a heterogeneous material with two phases: cement matrix and aggregates. One of its limitations is the great difference between tension and compression behaviors. Another limitation is the fragility, mainly under tensile stresses. Thus, reinforced concrete has complementary tensile resistance and additional ductility, given by steel bars or fibers (Bitencourt Jr et al. [6]).

The distribution of fibers in the concrete mixture is random, but the direction of casting intervenes considerably on distribution. Because of this, the fiber reinforced concrete is anisotropic.

There are various types of fibers: vegetal, polymeric, carbon, glass, steel, among others [9,10]. Steel fibers can take various shapes, surfaces and cross-sections.

Some fiber attributes must be considered:

- Shape: wavy or hooked fibers grant more pullout resistance than straight fibers.
- Surface: rough fibers grant better grip than plain fibers, due to greater contact surface to the matrix.
- Content: as more fibers, more resistance. However, the cost increases, and the workability is impaired.
- Cross section: as greater the area, greater the strength; as greater the perimeter, better the grip (more contact area between the fiber and the matrix).
- Length: longer fibers are better, but not as long, otherwise they break more easily. Too short fibers have low pullout resistance (Figueiredo [2]).
- Aspect ratio: the bigger, the more strength (Singh [14]).

### 2.2 SFRC Performance

The main advantage of the fiber is to guarantee tensile resistance after cracking starts, and to increase the tensile strength (FIB [13]). The fibers modify the stress-strain diagram mainly after the peak; in other words, they act after the beginning of cracking. They do not prevent nor delay the cracking, but lessen its effects. Figure 1 shows how fibers reduce the stress concentration at the end of a crack.

The stress-strain diagram for compression before the peak (pre-crack) undergoes little changing with the addition of fibers, because the latter act when the cracking begins. In Fig. 2, the curves for conventional concrete and fiber reinforced concrete practically coincide until the peak. After the peak, the area under the curve is greater for the fiber reinforced concrete (more strength). There is not a vertical extension (does not increase in compressive resistance), but a horizontal extension (post-cracking ductility). According to Kosmatka et al. [5], the fibers decrease the width of cracks and favor the branching of cracks, instead a straight propagation.

The concrete begins to crack at low tensile stresses. The steel fiber behaves just as the steel reinforcement bar. Since the steel resists highly to tensile stresses and is ductile, the combination of concrete and steel fiber modifies the stress-strain diagram. The peak stress increases, so there is an addition of tensile strength compared to the plain concrete. If the fiber content is less than the critical content (Figueiredo [2]), the strain softening behavior occurs

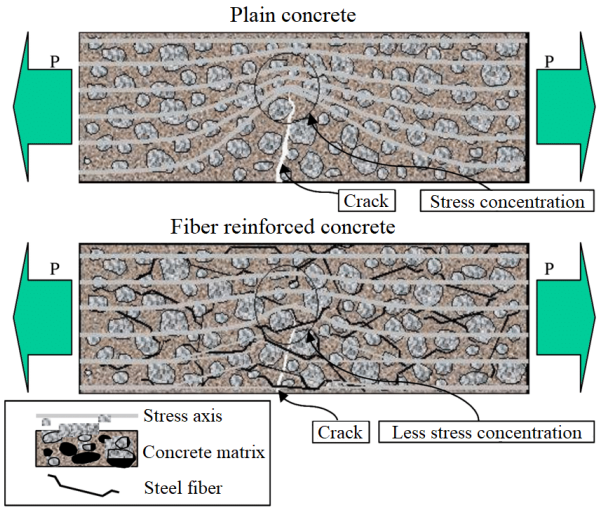


Figure 1. Stress concentration decreasing due to fibers (adapted from Figueiredo [2])

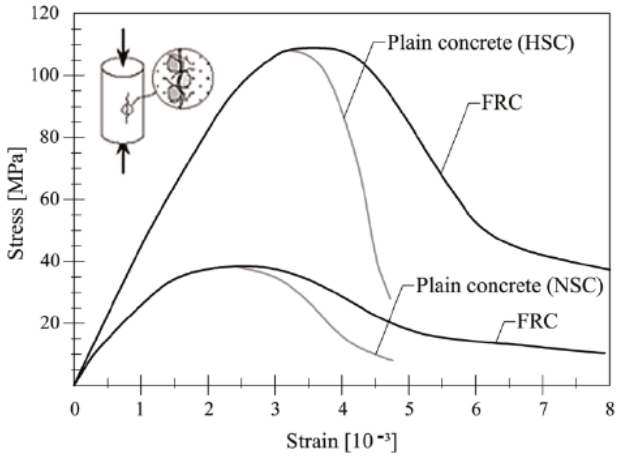


Figure 2. Comparation between conventional concrete and fiber reinforced concrete under compression (adapted from FIB [13])

after cracking. If the fiber content is greater than the critical content, the strain hardening is observed.

Before cracking, the flexural behavior is linear-elastic. When the first crack opens, stresses rearrange themselves and the neutral axis moves toward the most compressed edge.

The cracks are initially small, but they increase with time and loading. Due to stress concentration, a plasticity flow may occur provoking loss of energy, dissipated by the cracks. As the structure cracks, the loading capacity and stiffness decrease – this highlights the non-linearity of the concrete. The cracking growth is observed with the increasing crack width, number or spread of the crack, among other effects. When a concrete structure is critically cracked, it suddenly collapses, due to the fragility. There are several factors that favor the collapse, for instance, the discontinuities at the cement paste, the empty spaces and the break of the interface mortar-aggregate (Kotsovos [15]).

### 2.3 Finite Element Method (FEM)

This work uses the Finite Element Method (FEM), in which the structure is discretized in smaller elements interconnected by nodes. The boundary conditions and external links are applied (respectively, supports and loads). According to Soriano and Lima [16], the more elements (e.g., the more refined the mesh of finite elements), the closer the model results converge to analytical solution.

To proceed with FEM, it is necessary to define shape functions. The chosen shape functions are Lagrange quadratic polynomials. And to observe the behavior of a structure, it is necessary to know the constitutive law of

the material. The hypothesis of stress plain state was adopted.

***Remark 1: Linear and nonlinear stiffness matrix***. The matrix of constitutive relations $[C]$ is ($\nu$ is Poisson ratio and $E$ is the Young modulus):

$$[C] = \frac{E}{(1-\nu^2)} \begin{bmatrix} 1 & \nu & 0 \\ \nu & 1 & 0 \\ 0 & 0 & \frac{1-\nu}{2} \end{bmatrix}. \tag{1}$$

The elementary stiffness matrix $[K]^e$ is calculated for each finite element [16,17]:

$$[K]^e = \int_0^V [B]^T [C][B] dV. \tag{2}$$

As the elementary stiffness matrices are calculated, the stiffness coefficients are located at the global stiffness matrix, coupling the elements. Imposed the boundary conditions, the calculation proceeds with Hooke's law. In this work, the element used is the nine-nodes isoparametric rectangular element. The shape functions are obtained by Lagrange polynomials.

The matrix $[B]$ contains the derivatives of the shape functions. Because the element is isoparametric, it is necessary to obtain the Jacobian determinant $|J|$ to associate global ($x$ and $y$) coordinates with isoparametric coordinates ($\xi$ and $\eta$). At stress plain state, thickness $t$ is constant; therefore, the integration is done in the element area.

$$[K]^e = t \int_{-1}^{1} \int_{-1}^{1} [B]^T [C][B] |J| d\xi d\eta. \tag{3}$$

Equation (3) is used to calculate numeric integration (Oñate [17]). This method consists in calculate the sum of values of a function in certain points, obtained by the Gaussian quadrature method. Adapting eq. (3) for numeric integration:

$$[K]^e = t \sum_{i=1}^{n} \sum_{j=1}^{n} \left[ [B(\xi_i, \eta_j)]^T [C][B(\xi_i, \eta_j)] |J| \right] W_i W_j. \tag{4}$$

***Remark 2: Nonlinear solution***. According to Bathe [18], this is how a nonlinear system of equations is solved:

$$[K(u)]u = r - f. \tag{5}$$

In eq. (5), $[K(u)]$ is the nonlinear stiffness matrix, $u$ is the displacement vector, $r$ and $f$ are, respectively, external and internal force vectors. In nonlinear analysis, as iterations are processed, internal forces converge to the external loading and the displacement increment approaches zero.

There are methods to solve nonlinear equations, for instance, full Newton-Raphson and modified Newton-Raphson method (Kotsovos [15]); the latter was chosen, as it requires less computational effort, since the stiffness matrix does not change with iterations, only with load steps.

At each iteration, the global displacement vector receives the displacement increment obtained by eq. (5). For the iteration $i > 0$ and the load step $j > 0$ (Bathe [18]):

$$K_{(i-1)}^{(j-1)} \Delta u_{(i)} = r^{(j)} - f_{(i)}^{(j-1)}; \tag{6}$$

$$u_{(i)}^{(j)} = u_{(i-1)}^{(j)} + \Delta u_{(i)}. \tag{7}$$

Like the stiffness matrix in modified Newton-Raphson method, the vector of external forces only varies with the load steps. In addition, the following initial conditions are the absence of displacements and internal forces at the beginning of a load step. When the difference between external and internal forces is less than the chosen tolerance, the next loading step is processed.

The linear behavior of a concrete structure is observed until the cracking begins. Thereafter, the structure's stiffness decreases and the matrix $K$ reorganizes to become compatible with the damaged structure. A function must be used to associate the constitutive law of the material with the damage. Despite the SFRC is an anisotropic material, without loss of generality, one considers as an isotropic one. A damaged element is under apparent stress $\sigma$, but corresponding to effective stress $\sigma_e$, given by eq. (8). The relative damage $D$ ranges from zero (fully integer element) to one (fully damaged element). The damage model of Mazars was chosen to simulate the progression of damage of the structure.

$$\frac{\sigma}{\sigma_e} = 1 - D. \tag{8}$$

## 3 Example

In this work, a finite element program was developed in Python language. The analyzed model is a concrete beam 3.00 m wide (2.70 m span) and cross section 1.00x0.20 m (same dimensions as the test by Blanco Álvarez et al. [8]), made of SFRC, without steel bars. The beam is isostatic and three displacements are restricted (two vertical and one horizontal). The two loadings are concentrated and monotonic. The chosen element is the 9-node Lagrangean, rectangular and isoparametric element. The roughest mesh has 960 elements and 4097 nodes. The geometry and loading configuration are shown at Fig. 3.

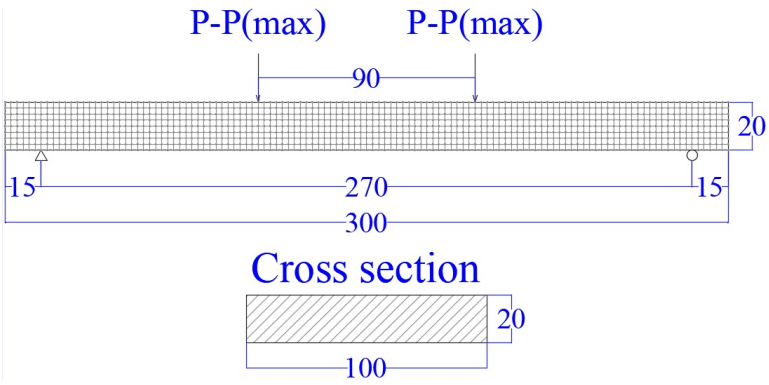


Figure 3. Scheme of the flexural four-point test, dimensions in centimeters (the Author)

The limit compressive stress adopted was 25 MPa (Concrete C25) (Blanco Álvarez et al. [8]). The steel fiber content adopted was 0.25% (Blanco Álvarez et al. [8]) and the Poisson ratio was adopted 0.2. The limit tensile stress was obtained by the eq. (9) according to ABNT [19]:

$$f_{ctm} = 0.3[f_{ck}]^{\frac{2}{4}}. \tag{9}$$

In eq. (9), $f_{ck}$ is the concrete compressive resistance in MPa and $f_{ctm}$ is the tensile resistance, also in MPa. For $f_{ck}$ = 25 MPa, a $f_{ctm}$ = 2.57 MPa was obtained. The Young modulus adopted was 28.5 GPa (average of 28 GPa (ABNT [19]) and 0.25% of steel fiber – 210 GPa).

Figure 4 shows a load-displacement diagram for loading steps of 5 kN. The number of elements in the mesh is equal to 960. The present solution is shown in blue thin line. For comparison, Fig. 4 also presents the results

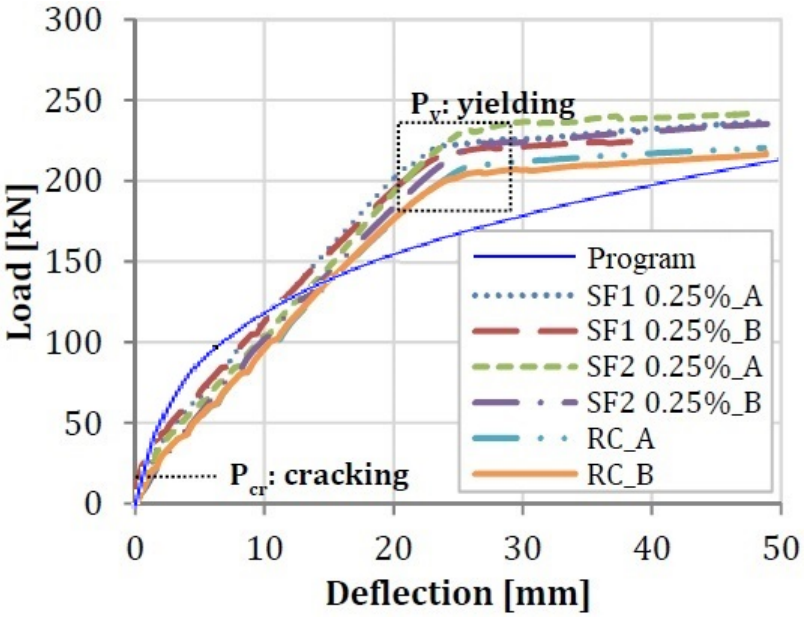


Figure 4. Load-displacement curves at the beam's middle point: results with bars reinforcements (Blanco Álvarez et al. [8]) and without steel bars (present work)

obtained by Blanco Álvarez et al. [8]. Despite the concrete and fiber materials are the same, (Blanco Álvarez et al. [8]) considers the concrete also reinforced with steel bars, which are not considered here.

Then, at Fig. 5, a map of damage for the mesh (with 960 elements) is showed, when the load is 100 kN. The black regions are undamaged zones ($D = 0$). Purple regions are slightly damaged. Medium damage is represented by shades of red and orange. Pale yellow zones are most damaged, whose damage $D$ approaches one.

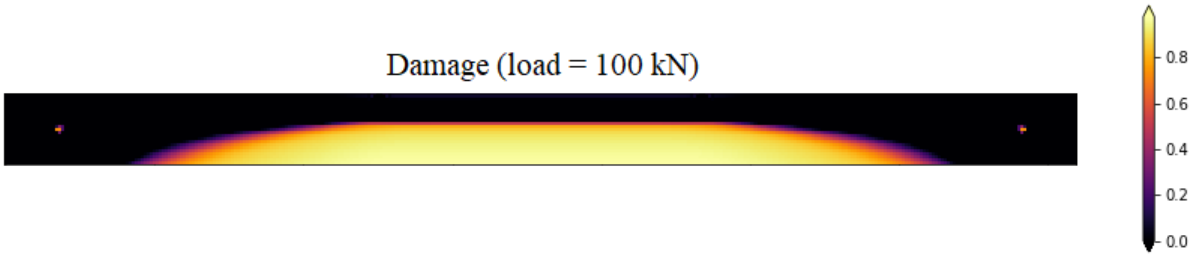


Figure 5. Damaged configuration of the mesh for a 100 kN load (the Authors)

## 4 Conclusions

Despite some differences between the numerical model developed in this work and the study made by Blanco Álvarez et al. [8], the results are near and validate the present approach. The main difference is that the present work has not modeled the reinforcement by steel bars such as it was presented in the experiment of Blanco Álvarez et al. [8]. However, as Fig. 4 shows, the numerical and experimental curves show the well job of fibers.

**Authorship statement.** The authors hereby confirm that they are the sole liable persons responsible for the authorship of this work, and that all material that has been herein included as part of the present paper is either the property (and authorship) of the authors, or has the permission of the owners to be included here.

## References

[1] A. Bentur and S. Mindess. *Fibre reinforced cementitious composites*. Crc Press, 2006.
[2] A. D. d. Figueiredo. *Concreto reforçado com fibras.* PhD thesis, Universidade de São Paulo, 2011.
[3] P. K. Mehta, P. J. Monteiro, and A. Carmona Filho. *Concreto: estrutura, propriedades e materiais*. Pini, 1994.
[4] O. Marchetti and M. H. C. Botelho. *Concreto armado-Eu te amo*, volume 1. Editora Blucher, 2015.
[5] S. H. Kosmatka, B. Kerkhoff, W. C. Panarese, and others. *Design and control of concrete mixtures*, volume 5420. Portland Cement Association Skokie, IL, 2002.
[6] L. A. Bitencourt Jr, O. L. Manzoli, T. N. Bittencourt, and F. J. Vecchio. Numerical modeling of steel fiber reinforced concrete with a discrete and explicit representation of steel fibers. *International Journal of Solids and Structures*, vol. 159, pp. 171–190, 2019.
[7] R. M. Jones. Mechanics of composite materials, taylor & francis. *Inc., USA*, vol. , 1999.
[8] A. Blanco Álvarez and others. Characterization and modelling of sfrc elements. vol. , 2013.
[9] H. Herscovici, D. Roehl, and E. d. S. Sánchez Filho. Estudo experimental de vigas curtas de concreto com fibras de aço sujeitas à flexão. *Revista IBRACON de Estruturas e Materiais*, vol. 12, n. 2, pp. 288–307, 2019.
[10] V. PASA. *Análise do comportamento de estruturas de concreto reforçado com fibras de aço via método dos elementos finitos*. PhD thesis, Dissertação (Mestrado em Engenharia de Estruturas), Universidade Federal do . . . , 2007.
[11] T. d. O. Abeche. *Modelagem computacional da interação dinâmica desacoplada entre viga e veículo considerando as irregularidades da via e a mecânica do dano contínuo*. PhD thesis, Dissertação de Mestrado, Pontifícia Universidade Católica do Paraná (PUCPR . . . , 2015.
[12] B. A. Opolski. *Simulação não linear física de vigas de concreto armado*. PhD thesis, Dissertação de Mestrado, Programa de Pós Graduação em Construção Civil e Estruturas, Universidade Federal do Paraná (UFPR . . . , 2019.
[13] FIB. Fib model code for concrete structures 2010, 2013.
[14] H. Singh. *Steel fiber reinforced concrete: behavior, modelling and design*. Springer, 2016.
[15] M. D. Kotsovos. *Finite-element modelling of structural concrete: short-term static and dynamic loading conditions*. CRC Press, 2015.
[16] H. L. Soriano and S. d. S. Lima. *Método de Elementos Finitos em Análise de Estruturas Vol. 48*. EdUSP, 2003.
[17] E. Oñate. *Structural analysis with the finite element method. Linear statics: volume 1: basis and solids*. Springer Science & Business Media, 2009.
[18] K.-J. Bathe. *Finite element procedures*. Klaus-Jurgen Bathe, 2006.
[19] N. ABNT. 6118 (2014). *Projeto de estruturas de concreto–Procedimento. Rio de Janeiro*, vol. , 2014.